



HAL
open science

Dual inhibition of BDNF/TrkB and autophagy: a promising therapeutic approach for colorectal cancer

Clément Mazouffre, Sophie Geyl, Aurélie Perraud, Sabrina Blondy,
Marie-Odile Jauberteau, Muriel Mathonnet, Mireille Verdier

► To cite this version:

Clément Mazouffre, Sophie Geyl, Aurélie Perraud, Sabrina Blondy, Marie-Odile Jauberteau, et al.. Dual inhibition of BDNF/TrkB and autophagy: a promising therapeutic approach for colorectal cancer. *Journal of Cellular and Molecular Medicine*, 2017, 21 (10), pp.2610-2622. 10.1111/jcmm.13181 . hal-01807807

HAL Id: hal-01807807

<https://unilim.hal.science/hal-01807807>

Submitted on 5 Jun 2018

HAL is a multi-disciplinary open access archive for the deposit and dissemination of scientific research documents, whether they are published or not. The documents may come from teaching and research institutions in France or abroad, or from public or private research centers.

L'archive ouverte pluridisciplinaire **HAL**, est destinée au dépôt et à la diffusion de documents scientifiques de niveau recherche, publiés ou non, émanant des établissements d'enseignement et de recherche français ou étrangers, des laboratoires publics ou privés.

Dual inhibition of BDNF/TrkB and autophagy: a promising therapeutic approach for colorectal cancer

Clément Mazouffre^{a, #}, Sophie Geyl^{a, #}, Aurélie Perraud^{a, b}, Sabrina Blondy^a, Marie-Odile Jauberteau^a, Muriel Mathonnet^{a, b, ##}, Mireille Verdier^{a, ##, *} 

^a Laboratoire EA 3842, Homéostasie cellulaire et Pathologies, Faculté de Médecine et de Pharmacie, Université de Limoges, Limoges Cedex, France

^b CHU de Limoges, Service de chirurgie digestive générale et endocrinienne, Limoges Cedex, France

Received: November 26, 2016; Accepted: March 4, 2017

Abstract

Colorectal cancer (CRC) is the most common digestive cancer in the Western world. Despite effective therapies, resistance and/or recurrence frequently occur. The present study investigated the impact of two survival pathways—neurotrophic factors (TrkB/BDNF) and autophagy—on cell fate and tumour evolution. *In vitro* studies were performed on two CRC cell lines, SW480 (primary tumour) and SW620 (lymph node invasion), which were also used for subcutaneous xenografts on a nude mouse model. In addition, the presence of neurotrophic factors (NTs) and autophagy markers were assessed in tissue samples representative of different stages. On the basis of our previous study (which demonstrated that TrkB overexpression is associated with prosurvival signaling in CRC cells), we pharmacologically inhibited NTs pathways with K252a. As expected, an inactivation of the PI3K/AKT pathway was observed and CRC cells initiated autophagy. Conversely, blocking the autophagic flux with chloroquine or with ATG5-siRNA overactivated TrkB/BDNF signaling. *In vitro*, dual inhibition improved the effectiveness of single treatment by significantly reducing metabolic activity and enhancing apoptotic cell death. These findings were accentuated *in vivo*, in which dual inhibition induced a spectacular reduction in tumour volume following long-term treatment (21 days for K252a and 12 days for CQ). Finally, significant amounts of phospho-TrkB and LC3II were found in the patients' tissues, highlighting their relevance in CRC tumour biology. Taken together, our results show that targeting NTs and autophagy pathways potentially constitutes a new therapeutic approach for CRC.

Keywords: colorectal cancer • neurotrophins • autophagy • therapy

Introduction

CRC represents the second cause of cancer-related mortality in developed countries [1]. In accordance with the UICC TNM classification [2], CRC is categorized into five stages (0–IV), which expand into several subdivisions according to the degree of severity and metastasis. Whereas surgery and chemotherapy are more efficient on low-grade stages, there is no curative treatment for patients with advanced-stage CRC, and mortality remains very high because of the resistance of cancer cells, resulting in treatment avoidance [3]. This aggressiveness could rely on uncontrolled growth factors pathway activation. Among them, neurotrophins (NTs), that is NGF, BDNF, NT3, NT 4/5, initially characterized in the nervous system [4], bind a specific high-affinity receptor—called Trk (tropomyosin receptor kinase) type A, B and C

respectively. Each subtype occurs as full-length (145 kD) or truncated (95 kD) forms. NTs primarily promote cell survival and differentiation [5] by activating either the PI3K/AKT (phosphatidylinositol 3 kinase/Akt) and/or MAPK (mitogenic activated protein kinase) and/or the PLC- γ (phospholipase C gamma) pathway [6]. TrkB expression and activation have been described for several types of cancers such as lymphomas, breast, lung cancers as reported by our team and others [7–14]. For CRC, we previously identified the BDNF/TrkB axis as a pro-survival pathway [7], as already been reported by Brunetto de Farias *et al.* [15]. Given its description as a potential target for anticancer therapy [16, 17], the use of the Trk inhibitor K252a [18] might result in the inactivation of Trk signaling and induce a cellular response including cell death [10, 19]. However, its effectiveness could be reduced by other cell survival mechanisms. Among these mechanisms, autophagy should be considered because it shares a common actor with TrkB signaling, the mTOR protein, downstream of the PI3K/AKT pathway.

Autophagy is a self-recycling process occurring in eukaryotic cells to maintain homeostasis under basal conditions which is greatly

[#]Equal contribution.

^{##}Equal contribution.

*Correspondence to: Mireille VERDIER
E-mail: mireille.verdier@unilim.fr

enhanced under stress [20]. It allows the degradation of altered cellular components *via* sequestration in autophagosomes, which merge with lysosomes to form the autophagolysosome [21, 22]. Several specific autophagic genes called *ATG* (Autophagy-related Genes) are involved in the active process. The most important are *ATG6* (called Beclin1 in mammals), *ATG5* and *ATG8*, called microtubule-associated protein light chain 3 or LC3 in mammals [23]. When LC3-I (cytosolic) combines with the autophagosome membrane, it is converted into the phosphatidylethanolamine-linked (PE) autophagosomal form — LC3II —, which is a commonly used autophagic marker [24, 25]. Although the precise role of autophagy in cancer remains ambiguous, it is considered as a prosurvival process, allowing cell retention under stress conditions (metabolic or oxidative) especially in late stages. [26]. Furthermore, autophagy could be responsible for the resistance of cancer cells to therapy, as already reported for CRC [26–28]. Therefore, its inhibition could assist in promoting cancer cell death [26–28] and represents a major challenge for the improvement of existing treatments [29,30]. Indeed, a recent study showed that inhibition of autophagy prevents the development and progression of CRC in patients [31].

The present study investigated the dual role of NTs and autophagy pathways in two CRC cell lines representative of different stages. The therapeutic potential of twin inhibition evidenced *in vitro* was checked and magnified *in vivo* on grafted animal. On the basis of our preliminary results, which confirmed the activation of both pathways in patients, this double therapeutic inhibition could be of considerable interest in the CRC treatment.

Materials and methods

Reagents and antibodies

K252a (Alomone Labs, Jerusalem, Israel), chloroquine (CQ) and rapamycin (Sigma-Aldrich, St. Quentin Fallavier, France) were used for NT, autophagy and mTOR inhibition, respectively. The primary antibodies used for Pan-AKT, phospho-AKT, mTOR, phospho-mTOR, Beclin-1, ATG5, LC3 and cleaved caspase-3 were obtained from Cell Signaling Technology (Saint Quentin Yvelines, France). Other primary antibodies were TrkB (BD Biosciences, Paris, France), phospho-TrkB (Millipore, Fontenay-Sous-Bois, France), BDNF (Santa Cruz Biotechnology, Heidelberg, Germany), PARP (Santa Cruz), VEGF (Abcam, Paris, France), Ki67 (Ventana-Roche, Meylan, France) and actin (Sigma-Aldrich).

Secondary antibodies were goat HRP conjugated with anti-rabbit IgG (Dako, Les Ulis, France) or with antimouse IgG (Dako). Others were dyed with Alexa Fluor 594 nm conjugated with anti-rabbit IgG (ThermoFisher Scientific, Waltham, MA USA) or with Alexa Fluor 488 nm conjugated with antimouse IgG. DAPI was purchased from Sigma-Aldrich.

Cell culture, transfection and treatments

SW480 and SW620 were obtained from American Type Cell Collection (ATCC/LGC promochem, Molsheim, France), authenticated by the seller

and cultured as previously described [7] in RPMI 1640 medium (Gibco Life Technologies, Paisley, UK). SW480 was a primary CRC-derived cell line (*i.e.* stage II), whereas SW620 was derived from the lymph node (*i.e.* stage III) of the same patient. Cells were used when they reached 80% subconfluence. Cell cultures were used for a maximum of 10 passages.

INTERFERIN transfection reagent (Polyplus; Cell Signaling Technology) was used for siRNA transfection. In total, 200,000 cells per well were transfected in 6-well plates with either 20 nM of negative control or ATG5 siRNA (Cell Signaling Technology). After 72 hrs with fresh medium, the cells were washed and recovered as described before. Silencing was confirmed by Western blotting.

Metabolic activity analysis

Metabolic activity was determined with the MTT assay (CellTiter 96 Aqueous One solution Cell Proliferation Assay, Promega, Charbonnières-les-Bains, France) following supplier instructions.

Apoptosis and necrosis analysis

The propidium iodide (PI) / Annexin-V-FITC double staining method was used as previously described [10] to determine early and late apoptosis as well as necrosis rates. Analyses were performed with a FACS Calibur flow cytometer (Becton Dickinson, Heidelberg, Germany).

Western blot analysis

After appropriate treatments, cells were collected, incubated for 15 min. at 4°C with RIPA lysis buffer, sonicated and centrifuged for 20 min. at 14,000×g at 4°C. Alternatively, 30 mg of tumoural tissue from patients or from engrafted mice were homogenized with ceramic bead in RIPA buffer, using Precellys mixer (MK 14 Precellys, Bertin Technology, Toulouse, France; 5500 rotations/sec.) and then centrifuged. Supernatants were collected, and the protein concentration was determined with the Bradford assay (Sigma-Aldrich). Western blot analysis was conducted as described before [7]. Band intensities were determined by densitometry using ImageJ software (NIH, Bethesda, MD, USA).

Indirect immunofluorescence

The experiments were realized as described previously [7] and analysed using confocal microscopy (LSM 510 META; Zeiss, Göttingen, Germany). Images were processed with the ZEN software application, and surface plots of the fluorescence data were generated with the image processing program ImageJ.

Quantitative RT-PCR

RNA extraction was performed with the RNeasy mini kit according to manufacturer recommendations (Qiagen, Courtaboeuf, France). A high-capacity cDNA reverse transcription kit (ThermoFisher) was used and PCR reactions were realized with TaqMan Fast Universal PCR Master

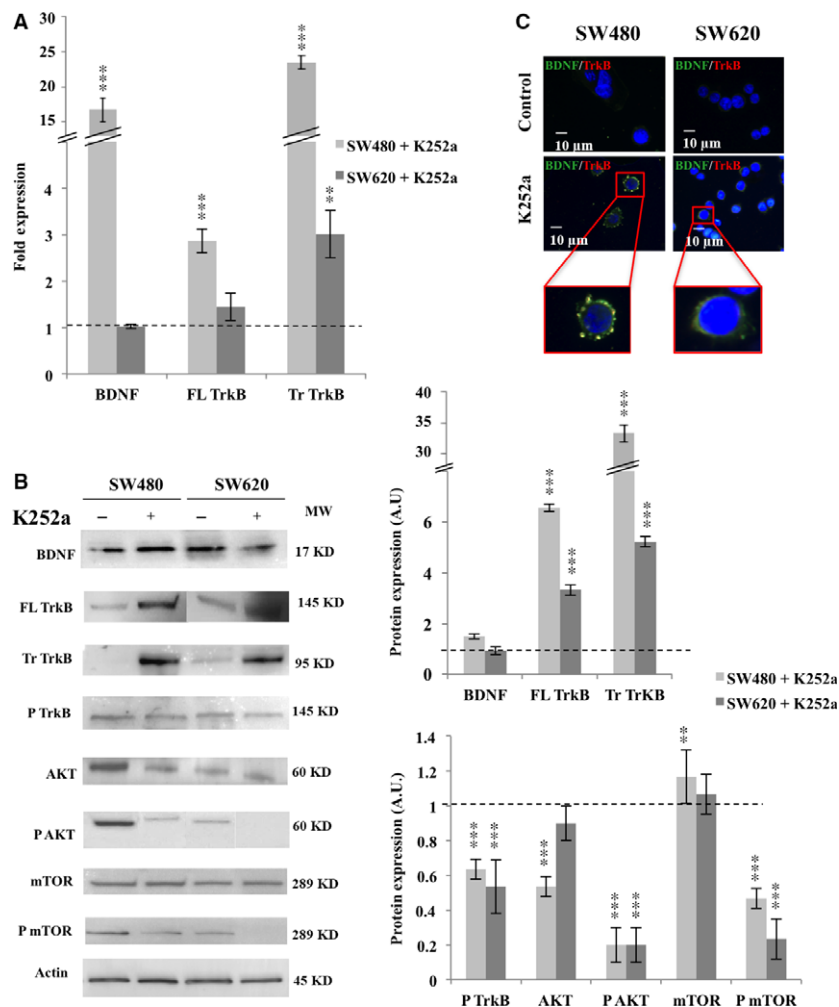


Fig. 1 Effect of tyrosine kinase receptor inhibitor (K252a) on TrkB/BDNF expression and autophagy induction. SW480 and SW620 were treated with 100 nM of K252a for 3 hrs, recovered, washed and total RNA and proteins were extracted (see Materials and methods). **(A)** BDNF, Full Length (FL) and Truncated (Tr) TrkB, transcripts expression was assessed by qPCR. Histograms are representative of three independent experiments. The fold expression was obtained by the comparative cycle threshold method using the GAPDH RNA expression level as internal control. **(B)** BDNF, FL TrkB, Tr TrkB, phospho-TrkB (P TrkB), AKT, phospho-AKT (P AKT), mTOR and phospho-mTOR (P mTOR), proteins expression were assessed by Western blotting. The density of each band representative for protein expression was calculated with ImageJ software. Images show representative results of three experiments. Statistically results are explained in comparison with control cells, normalized at 1 ($*P < 0.05$; $**P < 0.01$; $***P < 0.001$). **(C)** Staining of SW480 and SW620 was realized with anti-BDNF antibody (green), anti-TrkB antibody (red) and DAPI (blue). Images were obtained through confocal microscopy (magnification $\times 1000$). **(D)** Beclin1, ATG5 and LC3 proteins expression was assessed by Western blotting after treatment with either K252a (100 nM, 3 hrs) or with CQ (25 μ M, 3 hrs). The density of each band representative for protein expression was calculated with ImageJ software. Images show representative results of three experiments. Statistically results are explained in comparison with control cells, normalized at 1 ($*P < 0.05$; $**P < 0.01$; $***P < 0.001$). **(E)** Staining of SW480 and SW620 was realized with anti-LC3 antibody (green) and DAPI (blue) through indirect immunofluorescence. Rapamycin (20 nM, 3 hrs) was used as a positive control for autophagy induction. Relative fluorescence quantification was accomplished by using a green surface plot with the ImageJ software application.

Mix (ThermoFisher) with appropriate primers and probes as described previously [7]. Results were obtained with the StepOnePlus Real Time PCR System (ThermoFisher). All cycle thresholds (Ct) were normalized to *HPRT1* transcripts, and the relative quantities were calculated (untreated cells *versus* treated cells).

Mice xenografts and treatments

All animal studies were conducted in accordance with the guidelines established by the regional Institutional Animal Care and Use Committee (Comité Régional d'Éthique sur l'Expérimentation Animale du

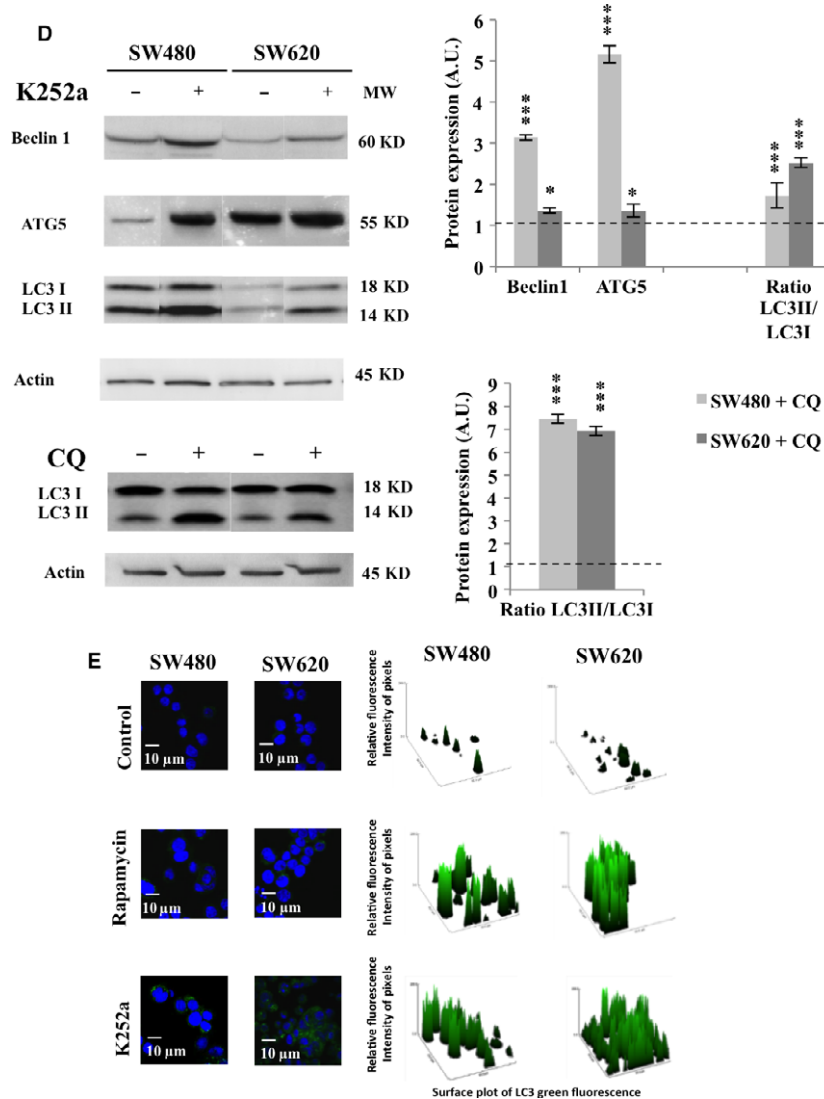


Fig. 1 Continued.

Limousin n°87-005). Seven-week-old female NMRI-nude mice (Janvier Labs, St Berthevin, France) were subcutaneously injected with 1×10^6 cells. Weekly length (L) and width (W) measurements were taken to track tumour growth, and the tumour volume was determined with the following formula: volume = $[L \times W(L + W)]\pi/12$.

Once the tumour volume reached 300 mm³ (day 0), mice were divided into groups (control, K252a, CQ, and K252a+CQ), with $n > 3$ mice per group. A physiological saline solution of K252a (0.5 mg/kg) was administered intraperitoneally every 3 days for 21 days as described in [32]. CQ was administered intraperitoneally (10 mg/kg) every 2 days for 12 days, following a modified version of the protocol used in [33]. Non-treated mice received a PBS injection every 3 days. At the end of the treatment, the animals were killed and the

tumours were divided one part for Western blot analysis and the other for histological analysis.

Histological analysis

Engrafted mice tumours were fixed in 10% formal before being dehydrated and included in paraffin following an automatic cycle (Anatomopathology department from the Limoges' Hospital). Four micrometre paraffin sections were realized and stained with haematoxylin-eosin-safran (HES), to evaluate necrotic areas. For proliferation rate assessment, Ki67 staining was performed as previously described [34] using BenchMark Technology (Ventana Medical Systems; Anatomopathology

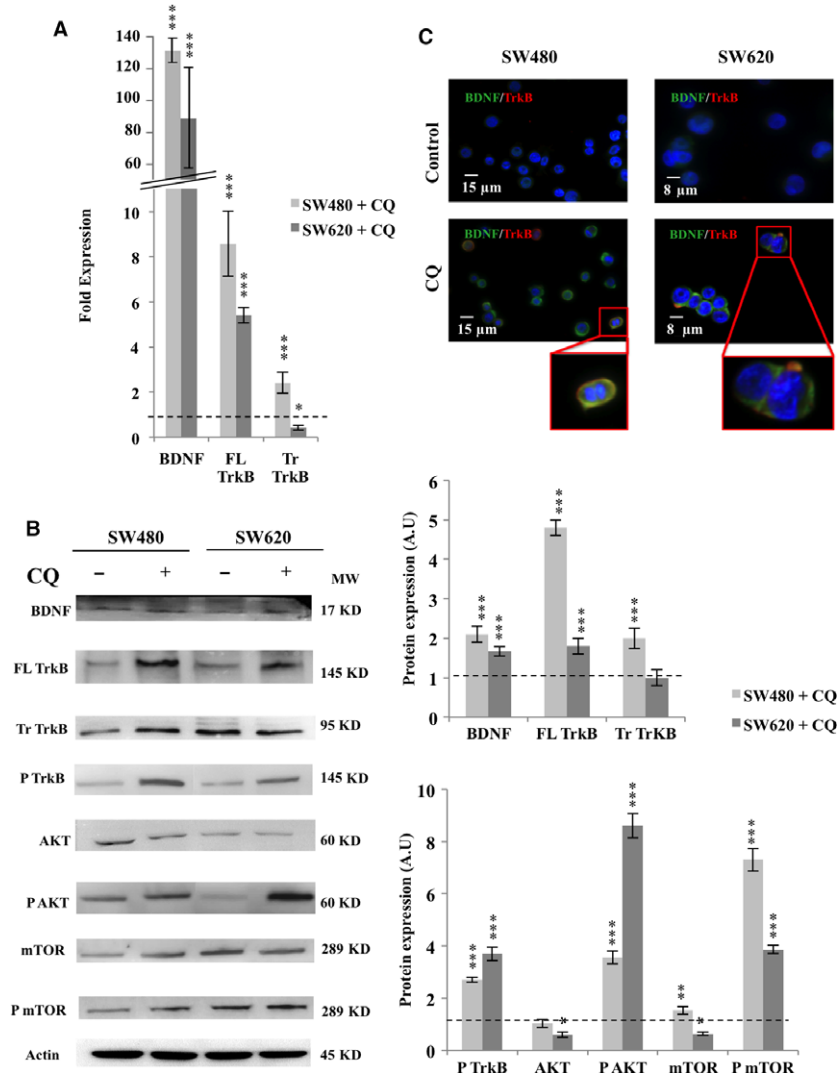


Fig. 2 Pharmacologic inhibition of autophagy with CQ induced TrkB/BDNF pathway activation in CRC cell lines. SW480 and SW620 were treated with 25 μ M of CQ for 3 hrs, recovered, washed and total RNA and proteins were extracted (see Materials and methods). **(A)** BDNF, FL TrkB and Tr TrkB, transcripts expression was assessed by qPCR as described in Fig 1 A. **(B)** BDNF, TrkB, phospho-TrkB, AKT, phospho-AKT, mTOR and phospho-mTOR proteins expression were assessed by Western blotting. The density of each band representative for protein expression was calculated with ImageJ software. Images show representative results of three experiments. Statistically results are explained in comparison with control cells, normalized at 1 (* P < 0.05; ** P < 0.01; *** P < 0.001). **(C)** Staining of SW480 and SW620 was realized with anti-BDNF antibody (green), anti-TrkB antibody (red) and DAPI (blue). Images were obtained through confocal microscopy (magnification \times 1000).

department from the Limoges' Hospital). Images were acquired with the Nanozoomer Digital Pathology 2.ORS software.

Patient samples

A total of 12 patients (men from 70 to 88 years old), who underwent CRC resection at Limoges University Hospital (France) between March 2011 and April 2014, were enrolled in this retrospective study, according to the Declaration of Helsinki. Exclusion criteria were applied as described before [35]. Tissue collection was approved by the local ethics committee ('Comité de Protection des Personnes, Sud Ouest Outre Mer'; CPP SOOM4; number DC-2008-604).

Statistics

All analyses were performed with Statview 5.0 software (Abacus Concepts, Piscataway, NJ, USA) and the ANOVA test. A P -value of <0.05 was considered statistically significant.

Results

Inhibition of BDNF/TrkB signaling induced autophagy in CRC cell lines

In a previous study, we demonstrated that CRC cells activate a survival and proliferative loop through BDNF/TrkB signaling [7]; here we investigated the consequences of NT inhibition in SW480 and SW620 cells cultured for 3 hrs with 100 nM K252a. As in these cell lines, we failed to detect TrkA and TrkC expression (neither transcripts nor proteins, data not shown and [7]), this pharmacological inhibitor mainly targeted TrkB signaling. Compared with control cells, a significant increase in the expression of BDNF transcripts (\times 16.8, P < 0.001), TrkB transcripts encoding the full length (145 kD, \times 2.9, P < 0.001) and the truncated form (95 kD, \times 24, P < 0.001) were observed in SW480 (*i.e.* CRC stage II)

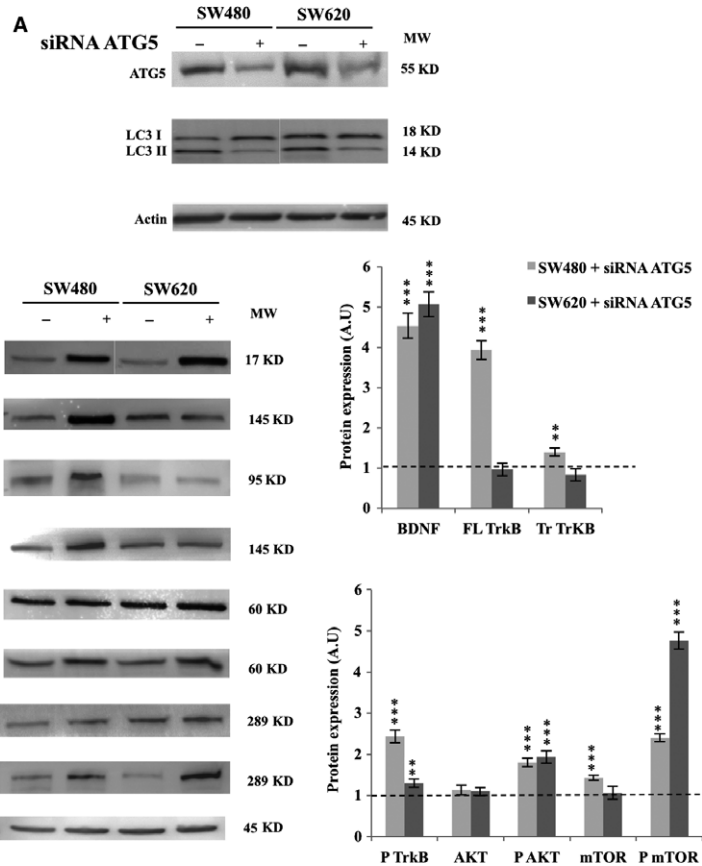


Fig. 3 siRNA-ATG5 inhibition of autophagy induced activation of the TrkB/BDNF pathway. SW480 and SW620 were transfected with siRNA ATG5, recovered, washed and total proteins were extracted (see Materials and methods). **(A)** To check silencing efficiency of siRNA, ATG5 and LC3 proteins expression were assessed by Western blotting. **(B)** BDNF, TrkB, phospho-TrkB, AKT, phospho-AKT, mTOR and phospho-mTOR expression were assessed by Western blotting. The density of each band representative for protein expression was calculated with ImageJ software. Images show representative results of three experiments. Statistically results are explained in comparison with control cells, normalized at 1 (* $P < 0.05$; ** $P < 0.01$; *** $P < 0.001$).

treated with K252a (Fig. 1A). For SW620 (*i.e.* CRC stage III), a similar significant enhancement was only observed for the truncated TrkB ($\times 3$, $P < 0.01$). Protein levels confirmed the qPCR results for both TrkB forms, in both cell lines (full length, $\times 6$ in SW480 and $\times 3$ in SW620, $P < 0.001$; truncated, $\times 35$ for SW480 and $\times 5$ for SW620, $P < 0.001$; Fig. 1B). The elevated transcription rate for BDNF observed for SW480 cell line was slightly confirmed by Western blot analysis (Fig. 1B). As both techniques evaluated intracellular BDNF, we assessed the secreted form and its ability to bind TrkB. BDNF quantification in the culture medium failed to exhibit significant variations between treated and control conditions in both cell lines (data not shown). However, colocalization of BDNF with TrkB was increased after K252a treatment, especially in SW480 cells (Fig. 1C), suggesting that BDNF was able to interact with TrkB, even in the presence of K252a. Nevertheless, this enhanced receptor expression as well as the BDNF/TrkB membrane colocalization failed to activate the downstream pathway, as evidenced by the decrease in phospho-TrkB, phospho-AKT and phospho-mTOR ($P < 0.001$ for both cell lines and for the three proteins, Fig. 1B), highlighting the inhibition of this pathway, which we expected to occur with K252a.

As we previously reported for glioblastoma (Jawhari *et al.*, 2016; manuscript in revision), autophagy can substitute to NTs signaling in a short time (< 24 hrs). Here, a decrease in mTOR phosphorylation

during K252a treatment (Fig. 1B) was compatible with autophagy activation. This result was accompanied by an increase in Beclin1 ($\times 3$, $P < 0.001$ for SW480; $\times 1.3$, $P < 0.05$ for SW620) and ATG5 expression ($\times 5$, $P < 0.001$ for SW480; $\times 1.2$, $P < 0.05$ for SW620; Fig. 1D). In addition, we demonstrated the conversion of cytosolic LC3 I into PE-linked LC3 II, one of the most widely used autophagic markers (LC3-II/LC3-I, $\times 2$ for both cell lines, $P < 0.001$; Fig. 1D). These results were confirmed through punctate localization of endogenous LC3 to autophagosomes with K252a treatment (Fig. 1E). By using an inhibitor of autophagic flow, CQ, we evidenced that autophagy was a functional process, as confirmed by an increased LC3II/LC3I ratio ($P < 0.001$ for both cell lines; Fig. 1D). In conclusion, during TrkB/BDNF inhibition, a functional autophagic process was activated. SW480 cells seemed to be more likely to undergo autophagy than SW620 cells. Because the inhibition of NTs signaling potentiated autophagy, we investigated whether the reverse was true and we explored the TrkB/BDNF activation when autophagy was inhibited.

Inhibition of autophagy induced BDNF/TrkB pathway activation in CRC cell lines

Autophagy was inhibited either pharmacologically with CQ or genetically with ATG5-siRNA. The use of CQ increased

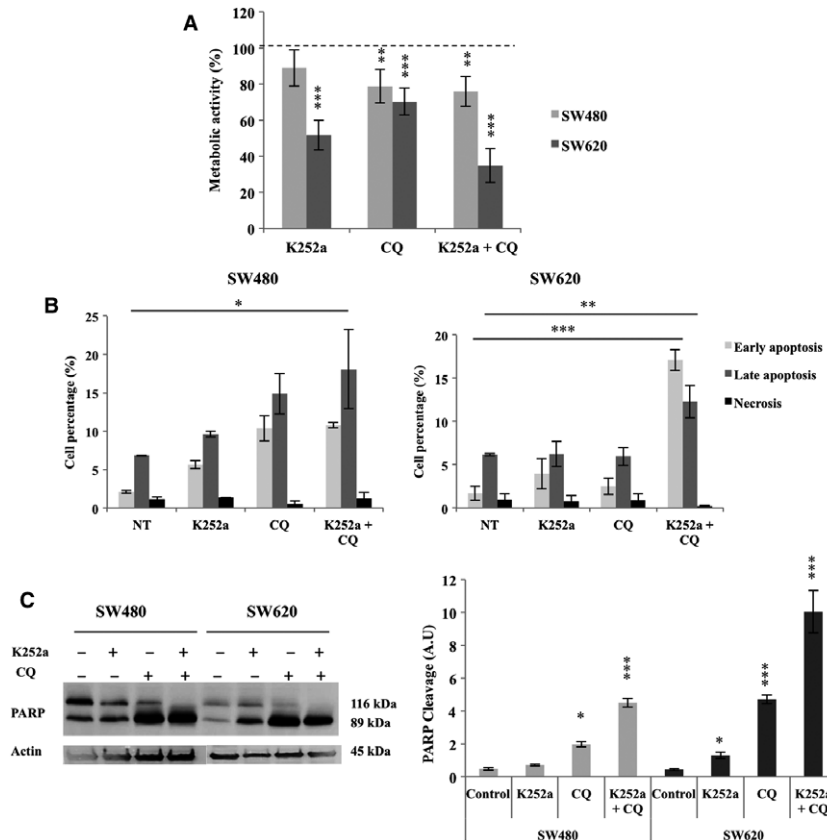


Fig. 4 Metabolic activity, cell death analysis and PARP cleavage in CRC cell lines after K252a, CQ and K252a + CQ treatments. SW480 and SW620 were treated with K252a, CQ or both molecules for 72 hrs (see Materials and methods). **(A)** Metabolic activity was assessed through MTT testing. Histograms show the means \pm S.E.M. of at least three independent experiments ($*P < 0.05$; $**P < 0.01$; $***P < 0.001$). **(B)** Apoptosis and necrosis were determined by PI/Annexin-V-FITC method with flow cytometry. Histograms show the means \pm S.E.M. of at least three independent experiments ($*P < 0.05$; $**P < 0.01$; $***P < 0.001$). **(C)** PARP cleavage was assessed by Western blotting. The density of each band representative for protein expression was calculated with ImageJ software. Images show representative results of three experiments. Statistically results are explained in comparison with non treated cells, normalized at 1 ($*P < 0.05$; $**P < 0.01$; $***P < 0.001$).

significantly BDNF and full-length TrkB transcripts regardless of the cell line (Fig. 2A), which was confirmed at the protein level for both proteins and cell lines ($P < 0.001$; Fig. 2B). Evaluation of secreted BDNF detected only slight enhancement in SW480 (data not shown), consistent with the ability of BDNF to bind to TrkB that we observed in both cell lines (Fig. 2C). The suggested downstream activation of the NTs signaling was confirmed by the increase of phosphorylated form of TrkB ($\times 2.5$ for SW480 and $\times 3.5$ for SW620; $P < 0.001$), AKT ($\times 4$ for SW480 and $\times 9$ for SW620; $P < 0.001$) and mTOR ($\times 7$ for SW480 and $\times 4$ for SW620; $P < 0.001$; Fig. 2B).

To avoid the potential side effects of CQ, autophagy was also inhibited using ATG5-siRNA. The efficiency of siRNA was assessed by the decrease in ATG5 expression and LC3-II/LC3-I ratio (Fig. 3A: loss of almost 60% for SW480 and 50% for SW620; $P < 0.001$). As observed with CQ, the genetic autophagy downregulation increased expression of BDNF ($\times 5$ for SW480 and SW620; $P < 0.001$), phospho-TrkB ($\times 2.4$ for SW480; $P < 0.001$ and $\times 1.2$ for SW620; $P < 0.01$), and the downstream effectors phospho-AKT (around $\times 2$ for SW480 and SW620; $P < 0.001$) and phospho-mTOR ($\times 2.5$ for SW480 and $\times 4.5$ for SW620; $P < 0.001$; Fig. 3B). These results emphasize that NTs signaling was activated when autophagy was blocked, thereby ensuring survival. Moreover, this relay seemed to be more loaded

in primary CRC-derived cell lines (*i.e.* SW480) because of the special expression enhancement of FL TrkB and phospho-TrkB ($P < 0.001$).

Targeting both the TrkB/BDNF and the autophagy pathways jeopardized CRC cell line survival

Because CRC cells used both the NTs and the autophagy to ensure their survival, dual inhibition was implemented to potentially sensitize cells to death. Although we failed to detect any change in cell fate after 3 hrs of treatment (data not shown), significant modifications were identified after 72 hrs (Fig. 4A). Even if the separate inhibition affected metabolic activity, it decreased more importantly with dual treatment (loss of 30% for SW480, $P < 0.01$, and loss of 65 % for SW620, $P < 0.001$). When evaluated the cell death pathway engaged by treated cells, we showed that the double pharmacological treatment significantly increased the apoptotic rate in both cell lines ($\times 2.7$ for SW480, $P < 0.05$ and $\times 3.7$ for SW620, $P < 0.001$), whereas the necrotic death remained stable (Fig. 4B). These results were corroborated by the large enhancement of PARP cleavage (Fig. 4C) observed in both cell lines when treated with K252a + CQ ($P < 0.01$).

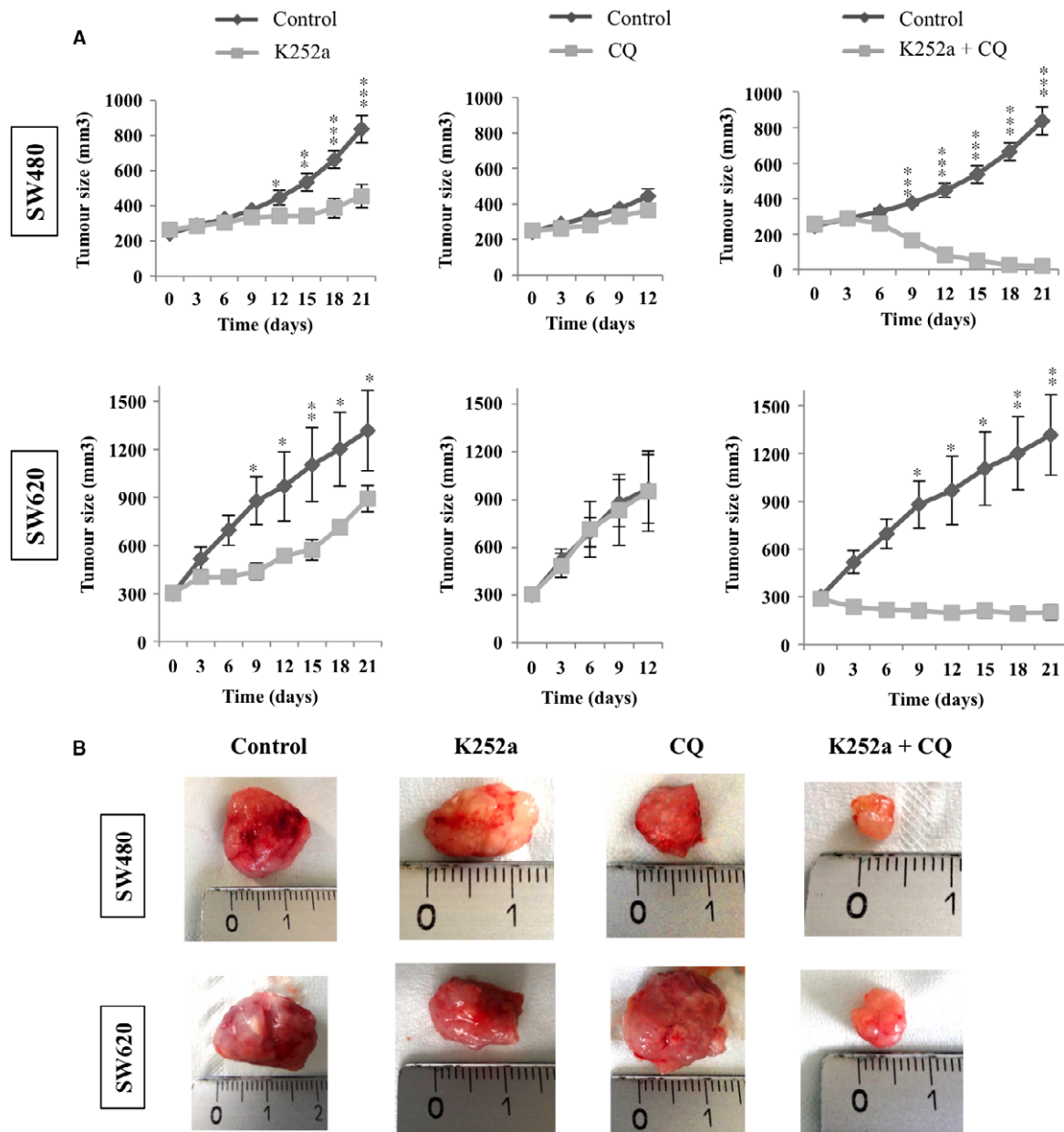


Fig. 5 Effects of NT inhibitor (K252a), autophagy inhibitor (CQ) and dual treatment on tumoural growth. Nude mice were subcutaneously engrafted with SW480 or SW620 (1.10^6 cells). When tumours reached a volume of 300 mm^3 , animals were divided into different groups and treated with K252a for 21 days or with CQ for 12 days or with both molecules (see Materials and methods). **(A)** Tumour growth was determined weekly. Results are expressed in mean tumour volumes (mm^3) \pm S.D. in comparison with the non treated group (* $P < 0.05$; ** $P < 0.01$; *** $P < 0.001$). **(B)** Representative images of tumours.

Dual inhibition of TrkB/BDNF and autophagy induced a spectacular decrease in tumour growth

Because the *in vitro* results indicated that dual inhibition was more effective than single inhibition, we checked efficiency of this dual

treatment on *in vivo* tumours developed in nude mice. The K252a significantly decreased tumour volume compared with control xenografts in both cell lines after 21 days of treatment (loss of 50%, $P < 0.001$ for SW480 and loss of 45%, $P < 0.05$ for SW620; Fig. 5A and B). On another hand, the CQ did not induce a significant decrease in tumour volumes even after 12 days of treatment. At the opposite,

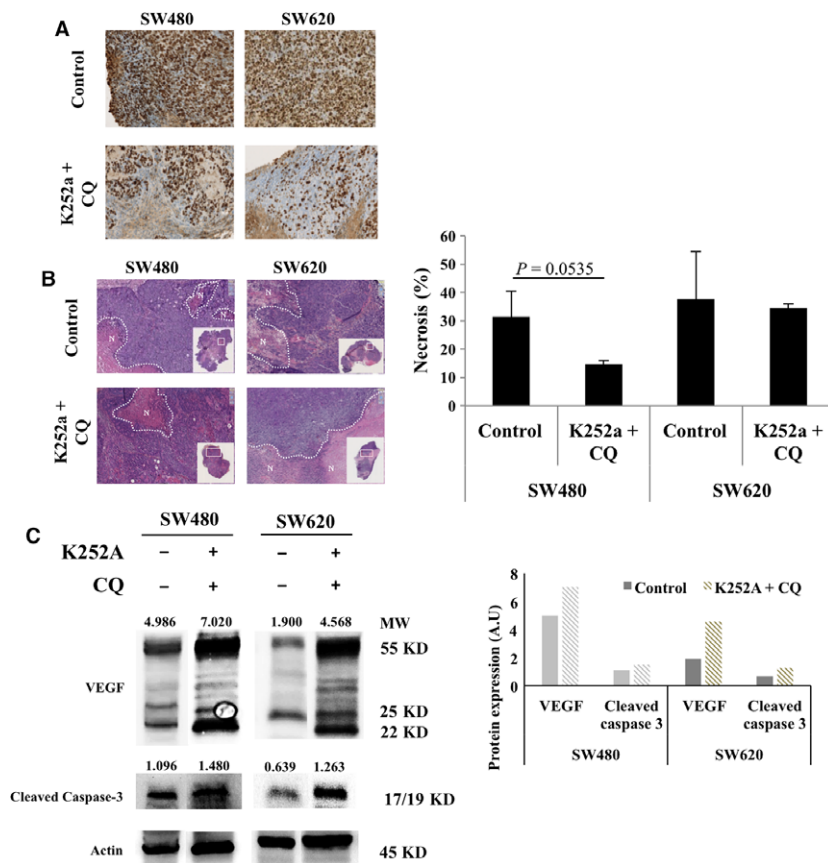


Fig. 6 Effects of dual treatment (K252a + CQ) on cell proliferation, cell death and vasculogenesis in tumour tissue originating from mice SW480 and SW620 xenografts. After being engrafted subcutaneously by SW480 or SW620, mice were treated by K252a + CQ as described in Materials and methods section. Tumour sample were collected from five xenograft mice for both cell lines. (A) Proliferation was determined by Ki67 immunostaining. Magnification was $\times 100$. (B) Necrosis was quantified using HES staining. Areas of necrosis are delimited by N. Magnification was $\times 50$. Results are representative of the ratio between necrosis area and total tumour area obtained with the Nanozoomer Digital Pathology 2.0RS (Hamamatsu) version 2.5.88 software. (C) Tumour sample were lysed and total protein were extracted. VEGF and cleaved caspase 3 were assessed by Western blotting. The density of each band was calculated with ImageJ software. Images show representative results performed for each condition, for both xenografts cell lines.

the dual inhibition induced a significant reduction in tumour volume compared with control after 21 days of treatment (decrease of 95% for SW480, $P < 0.001$, and of 75% for SW620, $P < 0.01$). More surprisingly, 40% of the tumours in the case of SW480 and of 25% of the tumours in the case of SW620 totally disappeared. Finally, tumours from SW480 xenografts were more sensitive to dual treatment than those from SW620 xenografts.

To delineate the mechanisms of tumour growth inhibition, we evaluated the relative rate of apoptosis and necrosis, as well as proliferation and angiogenesis by the mean of cleaved caspase 3 expression, HES and Ki67 staining and VEGF expression, respectively (Fig. 6). In both cell line engrafted tumours, we observed a proliferation decrease, as indicated by Ki67 expression reduction, when animals were double treated by K252a + CQ compared to controls (Fig. 6A). As HES staining revealed necrotic areas (Fig. 6B), we quantified the relative extent of the mechanism (Fig. 6B). Whereas the rate remained stable in SW620 engrafted tumours, it fell in double treated SW480 engrafted tumours, being borderline with significant threshold ($P = 0.0535$). Such observation could be explained by the great sensitivity of this cell line engrafted tumour, where we even observed a disappearance of some tumours. In the remaining tissue, necrotic areas could have been partially eliminated by host reaction. Furthermore, evaluation of apoptosis by cleaved caspase 3 expression showed a great

increase in both cell lines engrafted tumours double treated compared to controls. Such results suggest that this cell death pathway was induced when autophagy and NT signaling were inhibited (Fig. 6C), corroborating *in vitro* data. Moreover, enhancement of VEGF expression with double treatment underlined the neo-vascularization frequently occurring in CRC cancer and was compatible with a greater treatment accessibility (Fig. 6C).

Relevance of neurotrophins and autophagy as potential targets in patients with CRC

To extend these results to patients with CRC, NTs and autophagy markers expression was evaluated in tissue samples obtained from different stage tumours (three patients per stage). An increase in phospho-TrkB and phospho-AKT was observed, highlighting the activation of these pathways (Fig. 7). Moreover, the phosphorylation rate seemed dependent on the stage of the CRC, with an increase observed for advanced stages, especially in stage III and stage IV ($P < 0.001$) compared to stage 0/I. In addition, the LC3II/LC3I ratio also varied depending on stage, exhibiting increases in advanced stages (Fig. 7). These data emphasize the specific high level of TrkB expression and activation, as well as the occurrence of autophagy in tumoural cells and corroborate

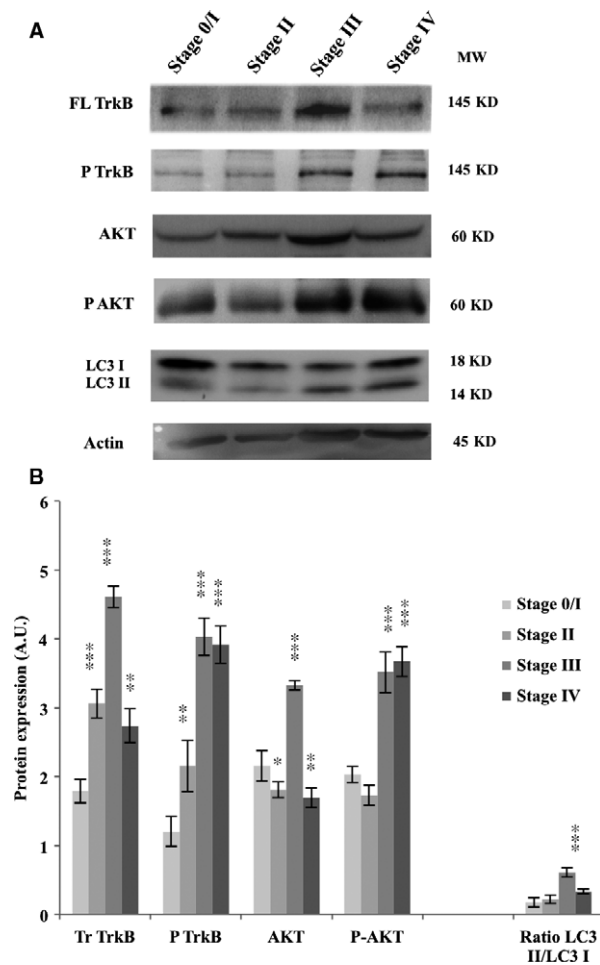


Fig. 7 Neurotrophin and autophagy pathways are active in patients with CRC. Tumour samples from each stage were collected from at least three patients with CRC, lysed and total proteins were extracted. FL TrkB, phospho-TrkB, AKT, phospho-AKT and LC3 protein expression was assessed by Western blotting. The density of each band was calculated with ImageJ software. Images show representative results of at least three experiments. Significant differences were obtained by comparison with Stage 0/I, considered as a pre-cancerous stage ($*P < 0.05$; $**P < 0.01$; $***P < 0.001$).

the potential role of these signaling pathways in CRC aggressiveness.

Discussion

Because CRC stays a world problem, new therapeutic targets are largely needed. This study focuses on inhibition of NTs (TrkB/BDNF) and/or autophagy, which are two survival-signaling pathways and shows the efficiency of the twin treatment, which largely contribute to reduce tumour growth (Fig. 8).

Overexpression of TrkB and BDNF constitute poor prognostic factors of tumour aggressiveness in various cancers [7, 10, 13, 36, 37]. This axis is also associated with the proliferation, migration and invasion in the case of peritoneal carcinomatosis [38] and constitutes an autocrine and paracrine loop survival in stress response, as we and others previously demonstrated in CRC [7]. In the present work, we used the pan-Trk inhibitor (K252a), in the primary CRC-derived cell line (SW480) and in the lymph-node-derived cell line (SW620). As both cell lines used in this work only expressed TrkB, this receptor signaling was the only one targeted. We observed the transcriptional and protein overexpression of TrkB and BDNF, which, even when binding together, failed to activate the AKT/mTOR pathway. This enhancement of both NT and receptor probably took place to try to restore this pathway. These results are consistent with previous reports, suggesting that K252a, although unable to block BDNF and TrkB interaction, is able to block downstream signaling [39]. In another tumoural model—Ewing sarcoma—, this inhibitor was responsible of a proliferation and survival loss of tumoural cells by targeting both TrkA and TrkB receptors, [19]. Even if the metastatic cell line SW620 showed comparable survival decrease, the reduced signaling in SW480 cells failed to induce a significant cytotoxicity, suggesting the involvement of a different cell survival process.

Among them, autophagy implication in CRC survival and in therapy resistance has already been shown [27, 28, 40, 41]. Here, we showed that inhibition of NTs with K252a resulted in activation of autophagy to ensure cell survival. A similar protective effect of autophagy has also been reported when the EGFR pathway is inhibited with erlotinib in non-small-cell lung cancer [42] or with anti-EGFR in CRC [43]. Moreover, we described a similar compensatory effect of autophagy in response to hypoxia when TrkC signaling was reduced in glioblastoma (Jawhari *et al.*, 2016, manuscript in revision). These results underscore the interplay between growth factors signaling (NTs) and autophagy.

Subsequently, we used either CQ, a classical autophagic flux-blocking molecule [41], or siRNA ATG5 (to counteract the well-known toxicity of CQ [44]) to test the reciprocal effect of autophagy inhibition on TrkB/BDNF signaling. Both approaches increased NTs transcripts and proteins expression as well as subsequent AKT/mTOR signaling, demonstrating the activation of this pathway. Therefore, autophagy inactivation induced the activation of the TrkB/BDNF survival pathway.

The dual inhibition of NTs and autophagy potentiated the effects of the single molecules *in vitro*, especially to induce apoptosis but also, in a spectacular way, *in vivo* on tumour growth. When analysing the mechanisms of inhibition of tumour growth, we observed that size reduction was mainly due to proliferation impairment and apoptosis potentialization in both cell line engrafted tumours. However, as shown with HES staining, necrosis also took place and we cannot absolutely rule out involvement of this pathway in tumour reduction. Similar positive effects of dual targeting efficiency have been described *in vitro* and *in vivo* [43–45]. For example, ongoing clinical trials already began in CRC, with the FOLFOX/bevacizumab/hydroxychloroquine study (clinical trial NCT01206530). Recently, the use of CQ was considered as an

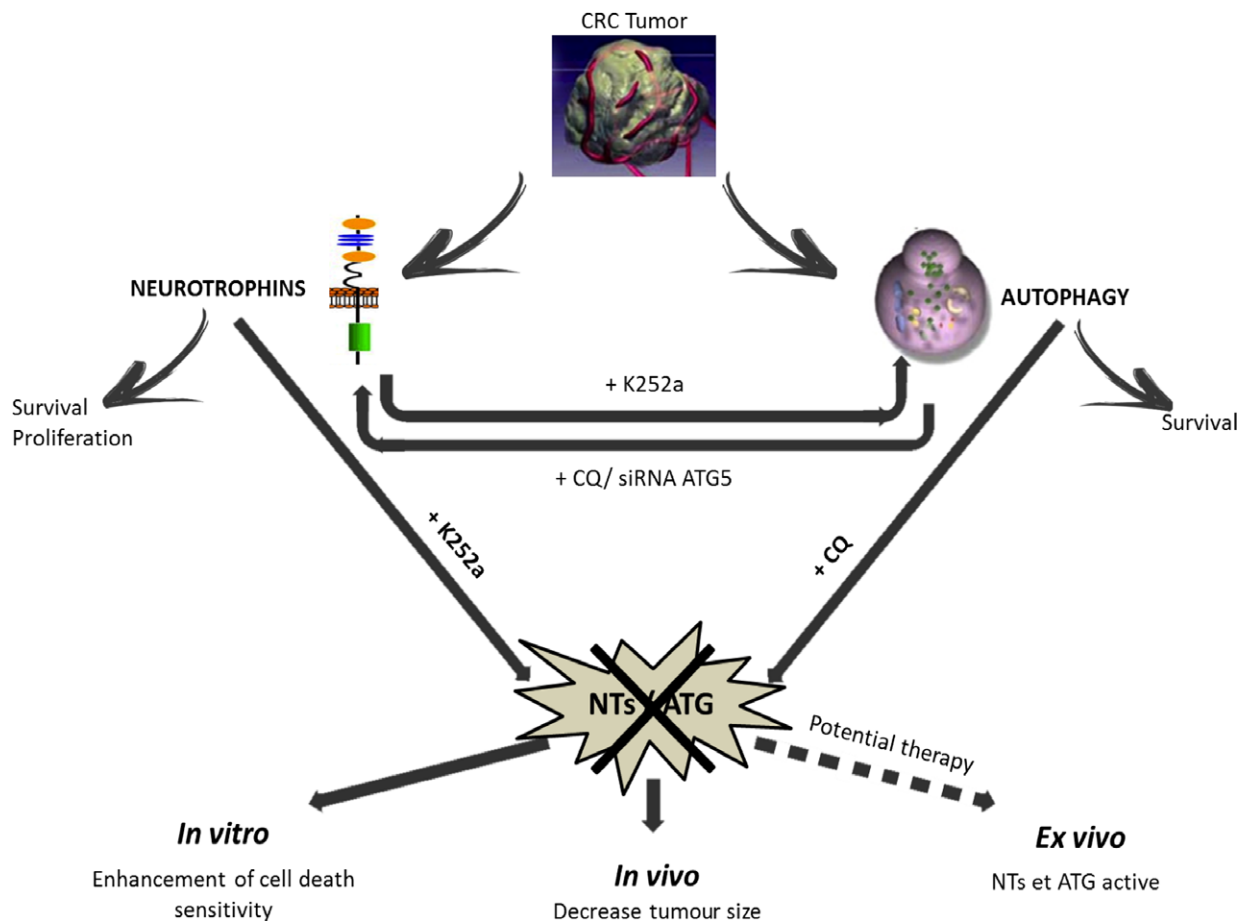


Fig. 8 Take home message. Whereas single NT or autophagy inhibition failed to sensitive CRC cells to death and induce activation of the reciprocal pathway, the dual inhibition prompted *in vitro* cell death, *in vivo* reduction of tumour growth, thus representing a promising new therapeutic approach.

adjunct to chemotherapy [46] and inhibition of autophagy is one last option to overcome the RTK resistance [47], reinforcing the use of dual inhibition to fight cancer.

Our study also revealed a difference between SW480 and SW620, already described in terms of morphology, BrdU labelling index and apoptosis susceptibility [48]. Especially we observed a higher level of basal TrkB and BDNF expression in primary tumour cells—SW480—than in metastatic cells—SW620—, that we and other previously reported [7, 49]. Furthermore, SW480 presents a more important autophagy basal rate than their metastatic counterpart. We hypothesized that the primary tumour cell line emphasizes both survival pathway in order to resist to a lower nutritional supply, due to defective vascularization frequently observed in primary tumour from which they come from [50]. In addition, relationship between TrkB expression and anoikis evasion, which supports distant metastasis, has already been published in CRC [49, 51]. This link could explain the behaviour difference in TrkB expression

between the two cells lines, as SW480 metastasis gave raise to SW620. This enhanced activation of both autophagy and NT pathways is in accordance with SW480 higher sensitivity to twin inhibition especially in engrafted tumours. So, targeting both autophagy and NTs in CRC primary tumours will be more effective, as observed *in vivo*. Moreover, an increased resistance of SW620 against treatments also suggests that other signaling pathways might be activated, in accordance with their capacity to adapt their behaviour to different environment (*i.e.* lymph node area).

Finally, the presence of phospho-TrkB and LC3II proteins was confirmed and increased with the stages of CRC in patient tissues. Because an excessive autophagic response was linked to metastasis and poor prognosis [52] and an increased TrkB expression enhanced the malignant potential in terms of proliferation, migration, invasion and anoikis inhibition in CRC cells [49], these two pathways constitute potential therapeutic targets, what our present study demonstrated.

Acknowledgements

C.M. received a fellowship from the Conseil Régional du Limousin and S.G. received a fellowship from the Agence Régionale de Santé Limousin (ARS). Additional financial support was provided by La Ligue Contre le Cancer (Comité du Limousin) and by Le Comité d'Orientation de la Recherche sur le Cancer (CORC) en Limousin. The funding institutions had no role in study design, data collection and analysis, decision to publish, or preparation of the manuscript. Authors are grateful to the Anatomopathology department from the Limoges' Hospital for histological and immunohistochemical

support, and to Michelle Nouailles for patients'informations. C.M., S.G., A.P. and S.B. performed the research; M.O.J., M.M. and M.V. designed the research study; M.M. and M.V. analysed the data; C.M., S.G., A.P. and M.V. wrote the paper.

Conflict of interest

The authors declare that they have no conflicts of interest with the contents of this article.

References

- Jemal A, Bray F, Center MM, *et al.* Global cancer statistics. *CA Cancer J Clin.* 2011; 61: 69–90.
- Obrocea FL, Sajin M, Marinescu EC, *et al.* Colorectal cancer and the 7th revision of the TNM staging system: review of changes and suggestions for uniform pathologic reporting. *Romanian J Morphol Embryol Rev Roum Morphol Embryol.* 2011; 52: 537–44.
- Housman G, Byler S, Heerboth S, *et al.* Drug resistance in cancer: an overview. *Cancers.* 2014; 6: 1769–92.
- Levi-Montalcini R, Cohen S. *In vitro* and *in vivo* effects of a nerve growth-stimulating agent isolated from snake venom. *Proc Natl Acad Sci USA.* 1956; 42: 695–9.
- Patapoutian A, Reichardt LF. Trk receptors: mediators of neurotrophin action. *Curr Opin Neurobiol.* 2001; 11: 272–80.
- Friedman WJ, Greene LA. Neurotrophin signaling via Trks and p75. *Exp Cell Res.* 1999; 253: 131–42.
- Akil H, Perraud A, Mélin C, *et al.* Fine-Tuning Roles of Endogenous Brain-Derived Neurotrophic Factor, TrkB and Sortilin in Colorectal Cancer Cell Survival. *PLoS One.* 2011; 6: e25097.
- Au CWH, Siu MKY, Liao X, *et al.* Tyrosine kinase B receptor and BDNF expression in ovarian cancers - Effect on cell migration, angiogenesis and clinical outcome. *Cancer Lett.* 2009; 281: 151–61.
- Bai H, Li H, Li W, *et al.* The PI3K/AKT/mTOR pathway is a potential predictor of distinct invasive and migratory capacities in human ovarian cancer cell lines. *Oncotarget.* 2015; 6: 25520–32.
- Dubonet L, Bentayeb H, Petit B, *et al.* Anti-apoptotic role and clinical relevance of neurotrophins in diffuse large B-cell lymphomas. *Br J Cancer.* 2015; 113: 934–44.
- Jia S, Wang W, Hu Z, *et al.* BDNF mediated TrkB activation contributes to the EMT progression and the poor prognosis in human salivary adenoid cystic carcinoma. *Oral Oncol.* 2015; 51: 64–70.
- Kim MS, Lee WS, Jeong J, *et al.* Induction of metastatic potential by TrkB *via* activation of IL6/JAK2/STAT3 and PI3K/AKT signaling in breast cancer. *Oncotarget.* 2015; 6: 40158–71.
- Sclabas GM, Fujioka S, Schmidt C, *et al.* Overexpression of tropomyosin-related kinase B in metastatic human pancreatic cancer cells. *Clin Cancer Res Off J Am Assoc Cancer Res.* 2005; 11: 440–9.
- Zhang P, Xing Z, Li X, *et al.* Tyrosine receptor kinase B silencing inhibits anoikis-resistance and improves anticancer efficiency of sorafenib in human renal cancer cells. *Int J Oncol.* 2016; 48: 1417–25.
- Brunetto de Farias C, Rosemberg DB, Heinen TE, *et al.* BDNF/TrkB content and interaction with gastrin-releasing peptide receptor blockade in colorectal cancer. *Oncology.* 2010; 79: 430–9.
- Akil H, Perraud A, Jauberteau M-O, *et al.* Tropomyosin-related kinase B/brain derived-neurotrophic factor signaling pathway as a potential therapeutic target for colorectal cancer. *World J Gastroenterol.* 2016; 22: 490–500.
- Roesler R, de Farias CB, Abujamra AL, *et al.* BDNF/TrkB signaling as an anti-tumour target. *Expert Rev Anticancer Ther.* 2011; 11: 1473–5.
- Tapley P, Lamballe F, Barbacid M. K252a is a selective inhibitor of the tyrosine protein kinase activity of the trk family of oncogenes and neurotrophin receptors. *Oncogene.* 1992; 7: 371–81.
- Heinen TE, Dos Santos RP, da Rocha A, *et al.* Trk inhibition reduces cell proliferation and potentiates the effects of chemotherapeutic agents in Ewing sarcoma. *Oncotarget.* 2016; 7: 34860–80.
- Mizushima N. The pleiotropic role of autophagy: from protein metabolism to bactericide. *Cell Death Differ.* 2005; 12: 1535–41.
- Han K, Kim J, Choi M. Autophagy mediates phase transitions from cell death to life. *Heliyon.* 2015; 1: e00027.
- Kroemer G, Mariño G, Levine B. Autophagy and the integrated stress response. *Mol Cell.* 2010; 40: 280–93.
- Lorin S, Codogno P, Djavaheri-Mergny M. Autophagy: a new concept in cancer research. *Bull Cancer (Paris).* 2008; 95: 43–50.
- Kabeya Y, Mizushima N, Ueno T, *et al.* LC3, a mammalian homologue of yeast Apg8p, is localized in autophagosome membranes after processing. *EMBO J.* 2000; 19: 5720–8.
- Klionsky DJ, Abdelmohsen K, Abe A, *et al.* Guidelines for the use and interpretation of assays for monitoring autophagy (3rd edition). *Autophagy.* 2016; 12: 1–222.
- Galluzzi L, Pietrocola F, Bravo-San Pedro JM, *et al.* Autophagy in malignant transformation and cancer progression. *EMBO J.* 2015; 34: 856–80.
- Burada F, Nicolini ER, Ciurea ME, *et al.* Autophagy in colorectal cancer: an important switch from physiology to pathology. *World J Gastrointest Oncol.* 2015; 7: 271–84.
- Sakitani K, Hirata Y, Hikiba Y, *et al.* Inhibition of autophagy exerts anti-colon cancer effects *via* apoptosis induced by p53 activation and ER stress. *BMC Cancer.* 2015; 15: 795.
- Sasaki K, Tsuno NH, Sunami E, *et al.* Chloroquine potentiates the anti-cancer effect of 5-fluorouracil in colon cancer cells. *BMC Cancer.* 2010; 10: 370.
- Wang J, Tan X, Yang Q, *et al.* Inhibition of autophagy promotes apoptosis and enhances anticancer efficacy of adriamycin *via* augmented ROS generation in prostate cancer cells. *Int J Biochem Cell Biol.* 2016; 77: 80–90.
- Lévy J, Cacheux W, Bara MA, *et al.* Intestinal inhibition of Atg7 prevents tumour initiation through a microbiome-influenced immune response and suppresses tumour growth. *Nat Cell Biol.* 2015; 17: 1062–73.

32. **Kawamura N, Kawamura K, Manabe M, et al.** Inhibition of brain-derived neurotrophic factor/tyrosine kinase B signaling suppresses choriocarcinoma cell growth. *Endocrinology*. 2010; 151: 3006–14.
33. **Lefort S, Joffre C, Kieffer Y, et al.** Inhibition of autophagy as a new means of improving chemotherapy efficiency in high-LC3B triple-negative breast cancers. *Autophagy*. 2015; 10: 2122–42.
34. **Mélin C, Perraud A, Christou N, et al.** New ex-ovo colorectal-cancer models from different SdFFF-sorted tumour-initiating cells. *Anal Bioanal Chem*. 2015; 407: 8433–43.
35. **Perraud A, Akil H, Nouaille M, et al.** Implications of cleaved caspase 3 and AIF expression in colorectal cancer based on patient age. *Oncol Rep*. 2012; 27: 1787–93.
36. **Fauchais A-L, Lalloué F, Lise M-C, et al.** Role of endogenous brain-derived neurotrophic factor and sortilin in B cell survival. *J Immunol Baltim Md*. 1950; 2008: 3027–38.
37. **Vanhecke E, Adriaenssens E, Verbeke S, et al.** Brain-derived neurotrophic factor and neurotrophin-4/5 are expressed in breast cancer and can be targeted to inhibit tumour cell survival. *Clin Cancer Res Off J Am Assoc Cancer Res*. 2011; 17: 1741–52.
38. **Tanaka K, Okugawa Y, Toiyama Y, et al.** Brain-Derived Neurotrophic Factor (BDNF)-Induced Tropomyosin-Related Kinase B (TrkB) Signaling Is a Potential Therapeutic Target for Peritoneal Carcinomatosis Arising from Colorectal Cancer. *PLoS One*. 2014; 9: e96410.
39. **Nye SH, Squinto SP, Glass DJ, et al.** K-252a and staurosporine selectively block autophosphorylation of neurotrophin receptors and neurotrophin-mediated responses. *Mol Biol Cell*. 1992; 3: 677–86.
40. **Sato K, Tsuchihara K, Fujii S, et al.** Autophagy is activated in colorectal cancer cells and contributes to the tolerance to nutrient deprivation. *Cancer Res*. 2007; 67: 9677–84.
41. **Yang Y, Hu L, Zheng H, et al.** Application and interpretation of current autophagy inhibitors and activators. *Acta Pharmacol Sin*. 2013; 34: 625–35.
42. **Li Y, Lam S, Mak JC, et al.** Erlotinib-induced autophagy in epidermal growth factor receptor mutated non-small cell lung cancer. *Lung Cancer Amst Neth*. 2013; 81: 354–61.
43. **Chen Z, Gao S, Wang D, et al.** Colorectal cancer cells are resistant to anti-EGFR monoclonal antibody through adapted autophagy. *Am J Transl Res*. 2016; 8: 1190–6.
44. **Janku F, McConkey DJ, Hong DS, et al.** Autophagy as a target for anticancer therapy. *Nat Rev Clin Oncol*. 2011; 8: 528–39.
45. **Cui J, Hu Y-F, Feng X-M, et al.** EGFR inhibitors and autophagy in cancer treatment. *Tumour Biol*. 2014; 35: 11701–9.
46. **Pascolo S.** Time to use a dose of Chloroquine as an adjuvant to anti-cancer chemotherapies. *Eur J Pharmacol*. 2016; 771: 139–44.
47. **Aveic S, Tonini GP.** Resistance to receptor tyrosine kinase inhibitors in solid tumours: can we improve the cancer fighting strategy by blocking autophagy? *Cancer Cell Int*. 2016; 16: 62.
48. **Hewitt RE, McMarlin A, Kleiner D, et al.** Validation of a model of colon cancer progression. *J Pathol*. 2000; 192: 446–54.
49. **Fujikawa H, Tanaka K, Toiyama Y, et al.** High TrkB expression levels are associated with poor prognosis and EMT induction in colorectal cancer cells. *J Gastroenterol*. 2012; 47: 775–84.
50. **Diaz-Cano SJ.** Tumour Heterogeneity: mechanisms and Bases for a Reliable Application of Molecular Marker Design. *Int J Mol Sci*. 2012; 13: 1951–2011.
51. **Fan M, Sun J, Wang W, et al.** Tropomyosin-related kinase B promotes distant metastasis of colorectal cancer through protein kinase B-mediated anoikis suppression and correlates with poor prognosis. *Apoptosis Int J Program Cell Death*. 2014; 19: 860–70.
52. **Giatromanolaki A, Koukourakis MI, Harris AL, et al.** Prognostic relevance of light chain 3 (LC3A) autophagy patterns in colorectal adenocarcinomas. *J Clin Pathol*. 2010; 63: 867–72.